Talanta 272 (2024) 125741

Contents lists available at ScienceDirect

Talanta

journal homepage: www.elsevier.com/locate/talanta

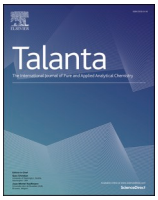

Development of a rapid aptamer-chemiluminescence sensor for detecting glyphosate pesticide residue in soybeans

Rui-Cian Weng [a,1], Min-Cheng Tsou [b,1], Jyun-Lin Lee [b], Chao-Ming Tseng [b,c], Yu-Fen Huang [d], Yu-Lin Xiao [b], Yen-Pei Lu [e], Wei-Chun Chou [f], Ruey-Feng Chang [a,g,**], Chun-Yu Chuang [b,*]

[a] Graduate Institute of Biomedical Electronics and Bioinformatics, National Taiwan University, Taipei, Taiwan
[b] Department of Biomedical Engineering and Environmental Sciences, National Tsing Hua University, Hsinchu, Taiwan
[c] Residue Control Division, Agricultural Chemicals and Toxic Substances Research Institute, Council of Agriculture, Executive Yuan, Taichung, Taiwan
[d] Institute of Analytical and Environmental Sciences, National Tsing Hua University, Hsinchu, Taiwan
[e] Instrument Research Institute, National Applied Research Laboratories, Hsinchu, Taiwan
[f] Department of Environmental Sciences, College of Natural and Agricultural Sciences, University of California, Riverside, CA, United States
[g] Department of Computer Science and Information Engineering, National Taiwan University, Taipei, Taiwan

ARTICLE INFO

Keywords:
Glyphosate
Aptamer
AuNPs
Chemiluminescence
Soybean

ABSTRACT

Glyphosate (GLY) is a widely used herbicide worldwide, particularly in cultivating genetically modified soybeans resistant to GLY. However, routine multi-residue analysis does not include GLY due to the complexity of soybean matrix components that can interfere with the analysis. This study presented the development of an aptamer-based chemiluminescence (Apt-CL) sensor for rapidly screening GLY pesticide residue in soybeans. The GLY-binding aptamer (GBA) was developed to bind to GLY specifically, and the remaining unbound aptamers were adsorbed onto gold nanoparticles (AuNPs). The signal was in the form of luminol-H_2O_2 emission, catalyzed by the aggregation of AuNPs in a chemiluminescent reaction arising from the GLY-GBA complex. The outcomes demonstrated a robust linear relationship between the CL intensity of GLY-GBA and the GLY concentration. In the specificity test of the GBA, only GLY and Profenofos were distinguished among the fifteen tested pesticides. Furthermore, the Apt-CL sensor was conducted to determine GLY residue in organic soybeans immersed in GLY as a real sample, and an optimal linear concentration range for detection after extraction was found to be between 0.001 and 10 mg/L. The Apt-CL sensor exploits the feasibility of real-time pesticide screening in food safety.

1. Introduction

As the global population continues to increase and the demand for food production rises, the use of pesticides is also on the rise to prevent large insect pests. According to statistics from the Food and Agriculture Organization of the United Nations (FAO) [1], global annual pesticide use increased from 2.2 to 4.1 million metric tons between 1990 and 2018, a trend that has persisted for the past 30 years. However, the environmental and food pollution caused by the abuse of pesticides has become a growing concern for public health.

Glyphosate (GLY), also known as N-(phosphonomethyl)-glycine, is a broad-spectrum systemic organophosphorus herbicide widely used in over 160 countries for the past 40 years. It is the active ingredient in all glyphosate-based herbicides (GBHs), including Roundup [2,3]. Notably, GLY-tolerant soybeans are the most widely cultivated genetically modified (GM) plant in the world. In 2011, approximately 90% of the 30 million acres of soybeans planted in the US were Roundup GM soybeans, and globally, Roundup GM soybeans accounted for 75% of total soybean production [4]. In 2015, the International Agency for Research on Cancer (IARC) of the World Health Organization (WHO) classified GLY as a Group 2A carcinogen, probably carcinogenic to humans [5]. The widespread use of GLY has been found to cause water pollution around

* Corresponding author. The School of Department of Biomedical Engineering and Environmental Sciences, National Tsing Hua University, No. 101, Sec. 2 Kuang-Fu Rd., Hsinchu 300, Taiwan.
** Corresponding author. The School of Graduate Institute of Biomedical Electronics and Bioinformatics, National Taiwan University, No. 1, Sec. 4, Roosevelt Rd., Taipei 106, Taiwan.
E-mail addresses: rfchang@csie.ntu.edu.tw (R.-F. Chang), cychuang@mx.nthu.edu.tw (C.-Y. Chuang).
[1] These authors contributed equally to this work.

https://doi.org/10.1016/j.talanta.2024.125741
Received 17 August 2023; Received in revised form 23 January 2024; Accepted 1 February 2024
Available online 8 February 2024
0039-9140/

farmland, and microscale residues of GLY have been detected in soil, air, surface water, and groundwater, as well as in breast milk and urine [6].

Aptamers have become widely used in scientific research, such as disease diagnosis, precision therapy, nanoscience, food safety, and environmental monitoring [7]. Nucleic acid aptamers are unique DNA or RNA molecules that fold into specific structures, such as hairpins or stem loops, and can specifically bind to target molecules [8]. Compared to proteins, aptamers have longer shelf life and thermal stability [9]. Four aptamers with a stem-loop structure isolated from the ssDNA database using SELEX technology have shown high affinity and specificity for binding to organophosphorus pesticides, including phorate, buffison, isocarbophos, and omethoate, with dissociation constants ranging from 0.8 to 2.5 μM [10]. Furthermore, nanomaterials, such as gold, silver, upconverting nanoparticles (UCNPs), carbon dots, and quantum dots exhibit potential for detecting pesticides owing to their high surface-to-volume ratio, physicochemical properties and target binding ability [11]. A highly sensitive aptamer-based colorimetric sensor was developed for Microcystin-LR (MC-LR) detection in real water samples [12]. The ABA aptamer binding to MC-LR with high affinity triggers a color shift of AuNPs in their plasma resonance absorption peaks upon binding the targets at high sodium chloride concentration.

Currently, pesticide residue detection in farming relies on the acetylcholine (ACh) biochemical rapid screening method, which requires pretreatment such as grinding the analyte and extracting residual pesticides. Although this method reduces detection time, it can only detect organophosphorus and carbamate pesticides and may produce inaccurate results due to matrix interference. Alternative methods have been developed to overcome the above limitations. The luminol-H_2O_2 chemiluminescence system is widely used in analysis and detection due to its low cost, wide linear range, and high sensitivity [13]. This system involves the reaction of luminol with hydroxide ions (OH^-) in an alkaline solution to form a double negative ion that can be oxidized by O_2 generated after the decomposition of H_2O_2. For instance, Hu et al. [14] used the luminol-H_2O_2 system to detect the organophosphorus pesticide quinalphos, achieving a linear relationship between luminescence intensity and pesticide concentration ranging from 0.02 to 1.0 mg/L, with a limit of detection (LOD) of 0.0055 mg/L. The average recoveries of quinalphos in tomato and green pepper samples were 97.20% and 90.13%, respectively.

Soybean-based foods are a staple in Asian cuisine and are increasingly recognized as a healthy alternative to animal products. In recent years, food safety has become a major concern for consumers, and therefore, the presence of GLY residue in soybeans is a matter of concern. However, routine multi-residue analysis does not include GLY due to the complex components of the soybean matrix, which require a separate extraction procedure for polar pesticides prior to determination using liquid chromatography-mass spectrometry (LC-MS).

Therefore, this study aimed to develop a highly sensitive and specific method for detecting GLY residues in soybeans. We used a specific GLY-binding aptamer (GBA) in combination with an AuNPs-catalyzed chemiluminescence reaction to develop an aptamer-based chemiluminescence (Apt-CL) sensor for detecting GLY pesticide residues in soybeans (Scheme 1).

2. Material and method

2.1. Preparation of GBA

The sequence of GLY-binding aptamer (GBA; 5′-AGC TTG CTG CAG CGA TTC TTG ATC GCC ACA GAG CT-3′ [10]) was synthesized by oligonucleotide purification cartridge (Genomics BioSci & Tech Co., Ltd, New Taipei City, Taiwan). The stock solution of GBA (100 μM) was dissolved in TE buffer and diluted to the 100 nM working solution, and stored at −20 °C. Before use, the GBA solution was heated at 90 °C for 10 min to unwind into single-stranded oligonucleotides [15].

2.2. Reagents and instrumentation

Chloroauric acid ($HAuCl_4{\cdot}4H_2O$) was procured from Thermo Fisher Scientific (Waltham, MA). Sodium citrate and sodium chloride were obtained from Sigma-Aldrich (St Louis, MO). Luminol was sourced from TCI (Tokyo, Japan). A luminol stock solution (25 mM) was prepared by dissolving 0.221 g of luminol in 1 mL of NaOH (5 M) and then diluting it to 50 mL with ddH_2O, which was subsequently stored at −20 °C. Working luminol solutions with a concentration of 0.5 mM were prepared. The working H_2O_2 solutions were freshly prepared from 30% (w/w) H_2O_2. The characteristics of AuNPs were determined through various methods: images captured using Transmission Electron Microscopy (TEM; JEOL JEM-F200 instrument; Peabody, MA), UV–visible absorption spectra obtained using an Agilent Technologies Cary 60 UV–Vis Spectrophotometer (Santa Clara, CA), and size distribution analysis conducted via dynamic light scattering (DLS; Malvern Panalytical Zetasizer Nano ZS; Worcestershire, UK).

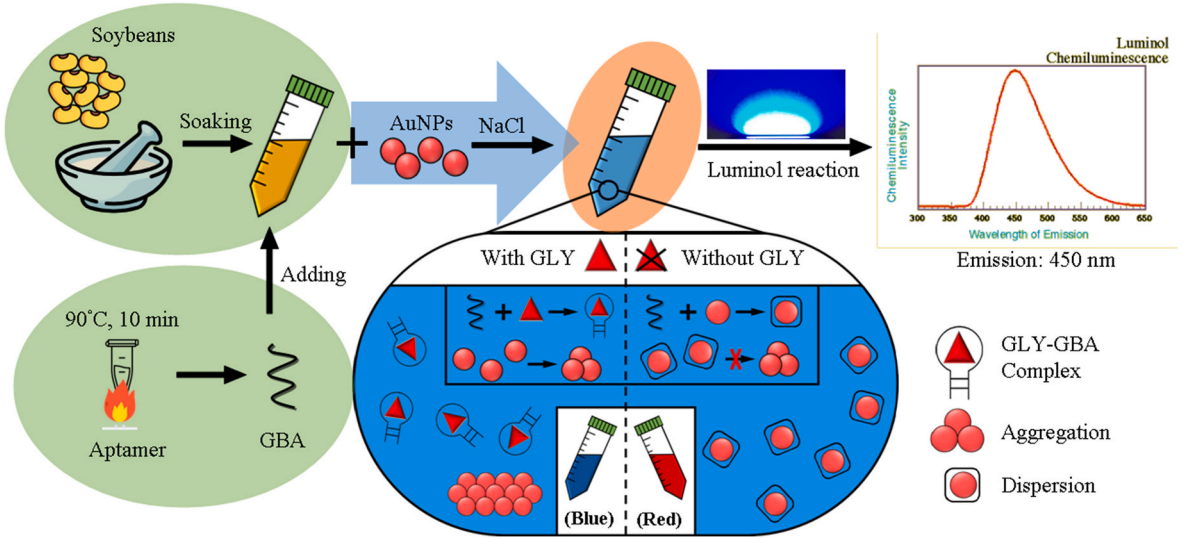

Scheme 1. Illustration of Apt-CL sensor employing the GBA aptamer on AuNPs to generate a luminol-H_2O_2 signal specificity for GLY residue screening in soybeans.

2.3. Synthesis of AuNPs

AuNPs were prepared by the classical citrate reduction method [16]. All glassware and stirrer were thoroughly cleaned in aqua regia (HNO_3–HCl = 1:3, v/v) for 5–10 min, rinsed in ddH_2O and dried in an oven to avoid interference from impurities. The 100 mL of $HAuCl_4 \cdot 3H_2O$ (1 mM) solution was heated to a boiling state, and 1 mL of sodium citrate solution (400 mM) was added while stirring for 8 min. The synthesis of AuNPs solution cooled to room temperature and stored at 4 °C.

2.4. Extraction of GLY in immersed-soybean sample

The organic and free-spraying soybeans (2 g) were immersed in a 15-mL polypropylene centrifuge tube with GLY solution (10 mg/L) at 4 °C for 1 h and dried in a chemical hood for 2 h. The QuEChERS extraction procedure for GLY in soybeans (Fig. 1) followed the guidelines outlined in the "Method of Test for Pesticide Residues in Foods – Multiresidue Analysis of Polar Pesticides and their Metabolites", as specified by the Taiwan Food and Drug Administration of the Ministry of Health and Welfare. The soybeans underwent the following process: (1) grinding, (2) placing 2 g in a centrifuge tube, (3) adding 10 mL of deionized water for 10 min, (4) adding 10 mL of a methanol solution containing 1% formic acid, immediately homogenizing in a high-speed homogenizer, followed by 5 min of agitation, (5) centrifugation at 5000*g* for 10 min at 15 °C, and finally (6) filtration through 0.22 μm PVDF membrane.

2.5. Chemiluminescence determination of GLY

The 100 μL of the extracted GLY solution was added with 100 μL of GBA solution (100 nM) and incubated for 15 min at room temperature. Subsequently, 100 μL AuNPs solution was added to the GLY-GBA solution and incubated for 10 min at room temperature to recognize the GLY-induced folding aptamer (e.g., hairpin structure). The 50 μL NaCl (3.5 M) was used to aggregate AuNPs. The CL reaction was triggered by infusing 100 μL of luminol-H_2O_2 solution (0.5 mM luminol:50 mM H_2O_2 4:1) into 60 μL of GLY-GBA-AuNPs solution. CL signals in a 96-well white plate were determined by a multi-detection reader in chemiluminescence mode (Synergy HT; Biotek, Winooski, VT) with an integration time of 1.0 ms, gain value of 150, and emission filter wavelength 460/40 nm.

2.6. LC-MS/MS analysis for GLY residue determination in soybeans

The GLY residue levels in soybeans were determined using LC-MS/MS. A Shiseido Capcell Pak ST column (150 × 2.0 mm ID, Shiseido; Tokyo, Japan) was employed for chromatographic separation at 40 °C, with an Agilent 1200 series high-performance liquid chromatography (HPLC) system (Agilent Technologies; Palo Alto, CA). Solvents included 50 mL methanol mixed with 940 mL ddH_2O and 10 mL formic acid (eluent A), and 990 mL methanol mixed with 10 mL formic acid (eluent B), all of HPLC grade. The gradient program was as follows: 0–9 min, 30% B at 0.2 mL/min; 9.5 min, 50% B at 0.2 mL/min; 11 min, 50% B at 0.4 mL/min; 18 min, 50% B at 0.4 mL/min; 19 min, 90% B at 0.4 mL/min; 22 min, 90% B at 0.4 mL/min; 22.1 min, 0% B at 0.2 mL/min; 30 min, 0% B at 0.2 mL/min. The volume injected was 5 μL. The molecular intensity was determined using a triple quadrupole mass spectrometer (Applied Biosystems 4000 QTRAP; Applied Biosystems, Warrington, UK) with the following features: ion-source: electrospray, positive mode; scan type: multiple reaction monitoring; ion-spray voltage: 3200; ion source temperature: 150 °C; curtain gas: 15; collision gas: high; nebulizer gas: 50; auxiliary gas: 60. Two transitions for GLY, 170/88 (declustering potential, DP: 16; collision energy, CE: 10) and 170/60 (DP: 16; CE: 16) were selected and used as the quantitative transition and the qualitative transition, respectively.

3. Results and discussion

3.1. Characterization of AuNPs in the presence of NaCl and aptamer

In this study, AuNPs were synthesized using the citric acid reduction method. As depicted in the TEM image, the average diameter of the AuNPs was found to be 13.1 ± 0.8 nm indicating a well-dispersed state (Fig. 2a; AuNPs alone). Upon the addition of 3.5 M NaCl, the AuNPs transformed from a dispersed form to an aggregated form (Fig. 2b; AuNPs-NaCl; 14.2 ± 0.9 nm). Additionally, the degree of dispersion of AuNPs was observed to be affected by the addition of GBA dissolved in TE buffer (salt) (Fig. 2c; AuNPs-GBA; 13.6 ± 1.1 nm). When GBA was first attached to the surface of AuNPs before the addition of NaCl, the aggregation of AuNPs was weakly dispersed (Fig. 2d; AuNPs-GBA-NaCl; 14.0 ± 1.2 nm). DLS analysis was also performed further to confirm the homogeneity and dispersibility of AuNPs in aqueous conditions, revealing a narrow size distribution with a mean diameter of 17.3 ± 5.5 nm (Fig. 2e). Even with the observed aggregation of AuNPs induced by

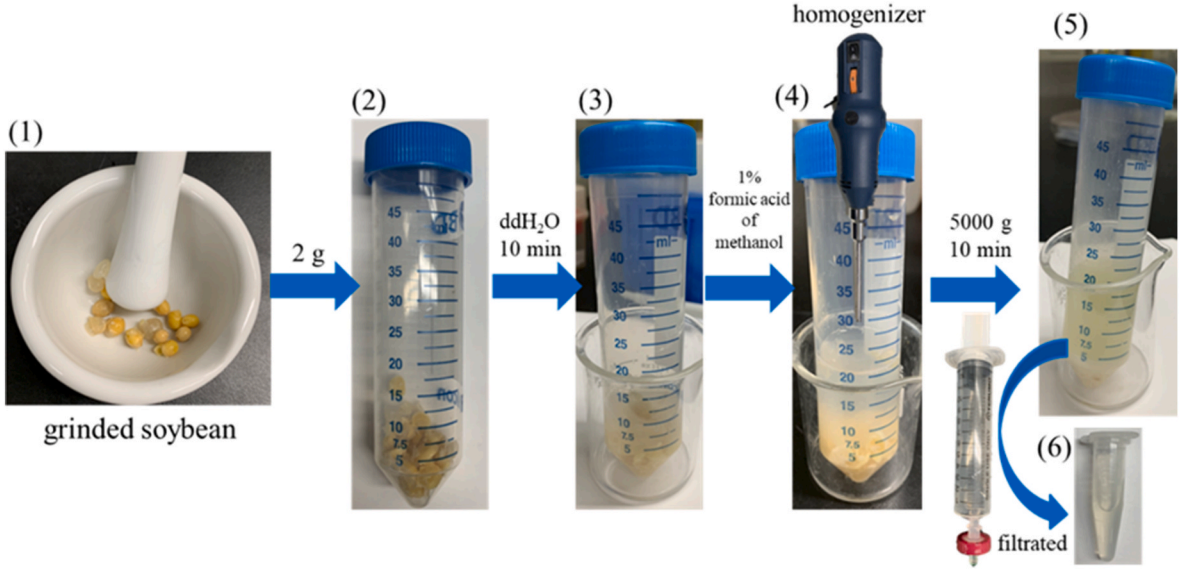

Fig. 1. Extraction procedure of GLY in soybean samples.

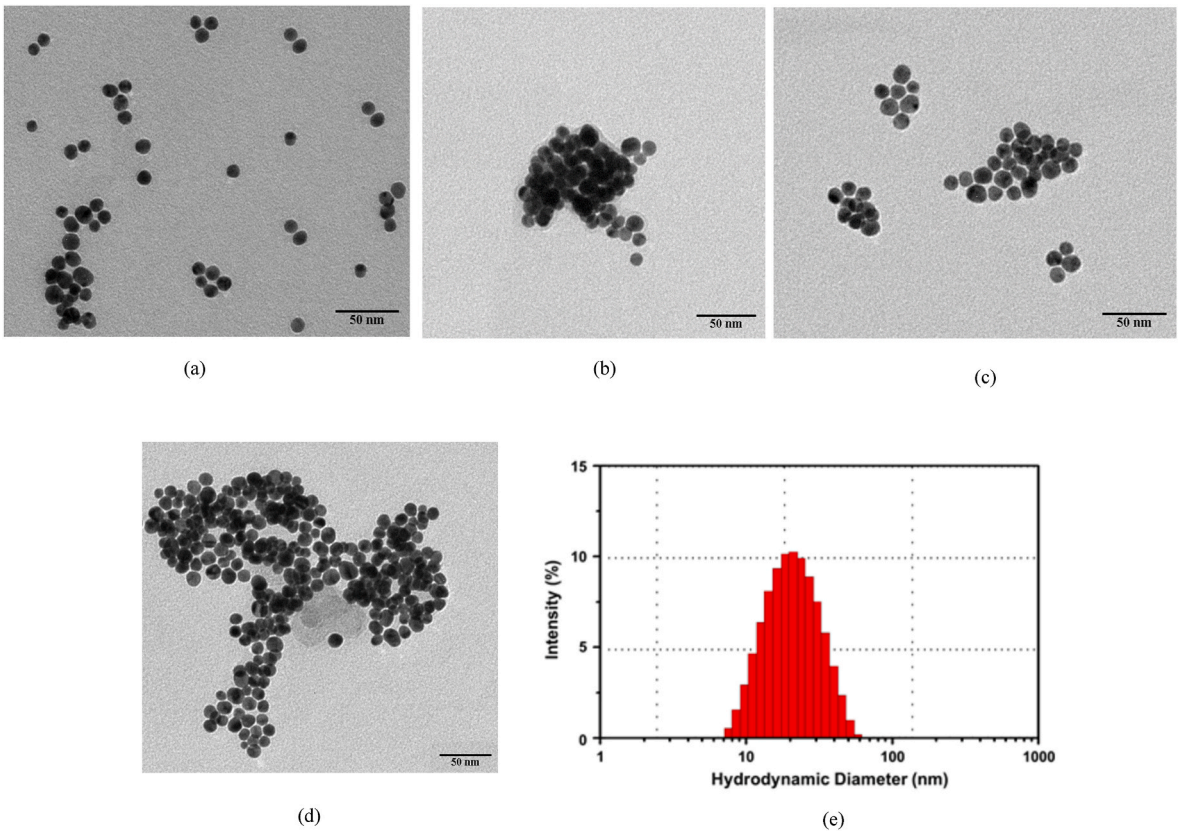

Fig. 2. Aggregation of AuNPs induced by NaCl and GBA aptamer coupling. The TEM images depicted the aggregation of (a) AuNPs alone, (b) AuNPs in the presence of NaCl (AuNPs-NaCl), (c) AuNPs coupled with the GBA aptamer (AuNPs-GBA), and (d) AuNPs modified with the GBA aptamer in the presence of NaCl (AuNPs-GBA-NaCl). (e) DLS diagram of the size distribution of AuNPs. The TEM images were captured at a magnification of 30,000×. The concentrations of NaCl and GBA were 3.5 M and 100 nM, respectively.

NaCl (Fig. 2b) or/and GBA aptamer coupling (Fig. 2c and d), the sizes of AuNPs under these conditions were shown no dramatic change.

3.2. Aggregation signals of AuNPs under NaCl and aptamer coupling

Under normal conditions, the AuNPs solution appeared red, with the highest characteristic absorption peak at 520 nm (Fig. 3a). When AuNPs were added to the NaCl solution, the color turned dark blue, and the absorption at the highest peak at 520 nm decreased while shifting towards a wavelength of 550 nm. This change indicated that the AuNPs had transformed from a dispersed state to an aggregated state due to the presence of NaCl (Fig. 2b). Upon the reaction of AuNPs with GBA, the characteristic peak of AuNPs at 520 nm remained (Fig. 3b). Following the addition of 3.5 M NaCl, the absorption value of the characteristic peak of AuNPs-GBA-NaCl decreased at 520 nm, and a peak shift to around 650 nm was observed. This observation indicated that the aptamer GBA did not influence the characteristic peak of AuNPs at 520 nm; it persisted even after NaCl addition. Therefore, the aptamer might resist the aggregation of AuNPs induced by NaCl.

It is known that NaCl can induce the aggregation of AuNPs and affect the color and light absorption of AuNPs solution [17]. The strong hydrophobic interaction and van der Waals force between nitrogen atoms in unfolded aptamers and AuNPs enable aptamers to bind to AuNPs in an unfolded structure without affecting the characterization of AuNPs [18].

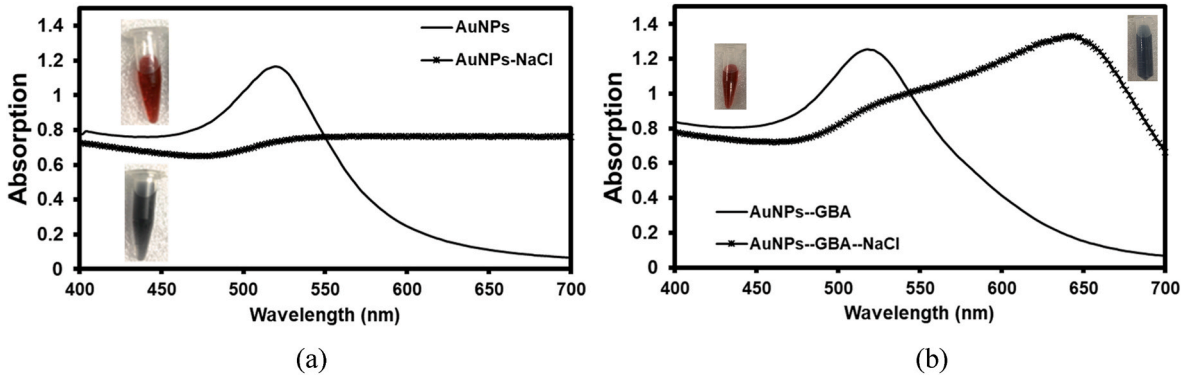

Fig. 3. Absorption spectra of AuNPs in the presence of NaCl and GBA aptamer. The absorption spectrum of (a) AuNPs and AuNPs-NaCl, and (b) AuNPs-GBA and AuNPs-GBA-NaCl. The absorption values of AuNPs in a NaCl solution (3.5 M) with a volume ratio of 2:1 for AuNPs to NaCl were measured using a UV/visible spectrometer in the range of 400–700 nm, with ddH2O used as a blank.

When the target is absent, the aptamer has a negatively charged phosphate backbone and exhibits an unfolded random coil-like structure, making it easily adsorb on the surface of AuNPs and resist the characteristics of salt-induced aggregation of AuNPs [19]. In contrast, when the aptamer is bound to the target, it transforms into a folded form in a relatively stable structure, making it less able to adsorb on AuNPs, and thus less able to resist the NaCl induction and promote the aggregation of AuNPs [20]. As mentioned above, when no target pesticide was present, the aptamer would adsorb on the surface of AuNPs to reduce the degree of AuNPs aggregation induced by NaCl. Conversely, when the aptamer was first bound to the target pesticide, the amount of adhesion on the surface of AuNPs decreased, which could not resist the NaCl induction and promote the aggregation of AuNPs. Therefore, this study has revealed that the distribution of AuNPs impacted the detection of pesticides. A higher degree of aggregation of the AuNPs led to a stronger luminescence signal intensity.

3.3. Catalytic activity of AuNPs on luminol-H_2O_2 reaction modulated by NaCl and aptamer coupling

To evaluate the stability of the colloidal solution and its effect on the catalysis of the luminol-H_2O_2 reaction in the chemiluminescence system, this study detected the potentials of negative charge densities in the states of AuNPs under NaCl and the GBA aptamer. The zeta potential results of AuNPs, AuNPs-NaCl, AuNPs-GBA, and AuNPs-GBA-NaCl were −39.9, −5.5, −24.1, and −11.2 mV, respectively (Fig. 4). This indicated that both salt (NaCl) and aptamer (GBA) can reduce the zeta potential on AuNPs. Zeta potential represents the surface charge properties of AuNPs, and their stability is affected by these properties [21]. The catalytic activity and surface charge of AuNPs are related to the luminol-H_2O_2 reaction in the luminescence system [22]. When the zeta potential is $\geq$ 30 mV or $\leq$ −30 mV, the AuNPs solution is observed in a stable dispersion state. Typically, for most nanocomposite materials, the Zeta potential falls within the range of 30–40 mV. In experimental settings, an exceeding Zeta potential of 30 mV widens the electrical double layer, leading to increased interparticle spacing and a dominance of repulsion over attraction. Consequently, stronger mutual repulsion occurs between particles, enhancing particle dispersion and system stability. Conversely, when the Zeta potential is 0 mV, particles have a tendency to aggregate, indicating the least stable state for a colloidal solution. Due to electrostatic repulsion effects, the anions luminol and HO^- in H_2O_2 are less likely to interact with stable AuNPs that possess a high surface negative charge density [23]. Hence, in this study, the AuNPs and aptamer-AuNPs exhibited comparable luminescence signals. The reduction in surface negative charge density of AuNPs caused by NaCl facilitated interactions with luminol and OH^- to the concurrent enhancement and stabilization of the luminescent signals.

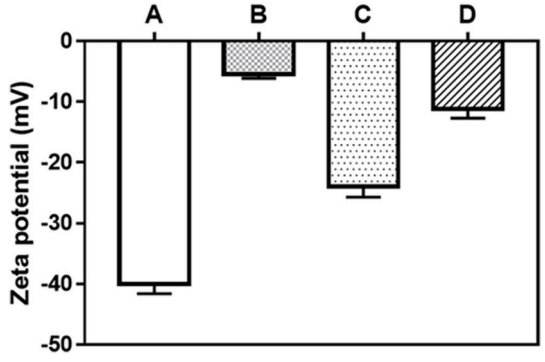

Fig. 4. Potential of AuNPs under NaCl and the GBA aptamer. Zeta potential of (A) AuNPs, (B) AuNPs-NaCl, (C) AuNPs-GBA and (D) AuNPs-GBA-NaCl.

3.4. Optimization of luminol-H_2O_2 reaction conditions in Apt-CL sensor

In this study, the chemiluminescence signal generated from the reaction of luminol with H_2O_2 was utilized to detect pesticide residue GLY. To optimize the Apt-CL sensor, the volume ratio of luminol-H_2O_2, pH value of luminol, and concentration of NaCl were investigated. The results indicated that the optimal luminescence signal was obtained at a volume ratio of luminol to H_2O_2 of 4:1 (80 μL and 20 μL, respectively), with a decrease in luminol intensity observed at higher volumes of H_2O_2 (Fig. 5a). The optimal volume ratio in this study (4:1) was more sensitive than that used in a previous study (2:1) [24]. The chemiluminescence intensity of the luminol-H_2O_2 reaction increased with pH, with the best luminescence signal observed at pH 14 (Fig. 5b), which was consistent with a previous study that reported the luminol-H_2O_2 chemiluminescence reaction usually occurring in strongly alkaline conditions [25]. Additionally, NaCl induced aggregation of AuNPs to blue color and affected the surface charge, thereby influencing the luminol-H_2O_2 reaction. The chemiluminescence intensity of the luminol-H_2O_2 reaction catalyzed by AuNPs aggregation degree induced by different NaCl concentrations was investigated. The reaction at 3.5 M NaCl concentration showed the best luminescence intensity (Fig. 5c). This study had confirmed the chemiluminescent signals primarily originated from the luminol-H_2O_2 system of AuNPs, aptamer, AuNPs-aptamer, and AuNPs-aptamer-(luminol-H_2O_2) (Fig. S1). In each case of AuNPs, aptamer, and AuNPs-aptamer, low chemiluminescent signals were observed, resembling the original background values. The results above indicate that the optimal conditions for the highest chemiluminescence intensity were 80 μL of luminol and 20 μL of H_2O_2 (v/v 4:1) (Fig. 5a), pH 14 (Fig. 5b), and a NaCl concentration of 3.5 M (Fig. 5c).

3.5. Detection of GLY using Apt-CL sensor

The chemiluminescence intensity of the GBA-GLY combination indicated a complete reaction within 15 min, which remained stable thereafter. Hence, the optimal binding reaction time was estimated to be 15 min (Fig. 6a). As luminol and H_2O_2 produced luminescence signals immediately, their luminescence intensity decreased with prolonged reaction time. The study found that luminol can last for about 30 min, necessitating detection of the luminol-H_2O_2 luminescent signal within 30 min. This study detected GLY under optimized conditions using GBA as a molecular probe. During detection, part of GBA was specifically bound to GLY while the rest was adsorbed on AuNPs surfaces. GLY concentrations displayed different abilities of luminol-H_2O_2 catalysis. The chemiluminescence intensity of GLY concentrations in the range of 0.10–1.0 × 10^4 μg/L exhibited a strong linear relationship (R^2 0.9965 and LOD 0.008 μg/L) (Fig. 6b). The LOD utilized in this study relies on equation 3.3σ/S, where σ denotes the standard deviation of response value of the blank solution, and S represents the slope of the corrected trend line [26].

The Apt-CL sensor developed in this study successfully utilized GBA to detect GLY, exhibiting a strong linear relationship between chemiluminescence intensity and GLY concentration. The detection range and LOD achieved by the Apt-CL sensor were lower compared to other aptamer detection methods (fluorescence and colorimetry). Aptamers are generally used as molecular probes to improve the specificity of detection, with most of them utilizing AuNPs to change the aggregation degree as a quencher in the inner filter effect (IFE), and then excite the fluorescent nanomaterials to emit signals. In both of previous studies, aptamers served as molecular probes, and fluorescent nanomaterials were utilized to emit light for GLY detection purposes. One method used a 6-carboxy-fluorescein-labeled aptamer attached to magnetic nanoparticles, tested in spiked lettuce and carrot samples, showing a linear decrease in fluorescence concerning GLY levels from 0.1 to 1 × 10^4 μg/L (LOD 0.088 μg/L) [27]. Another approach involving surface-enhanced Raman scattering (SERS) utilized the polycondensation of melamine and p-benzaldehyde (MaBd) in combination with a GLY aptamer to

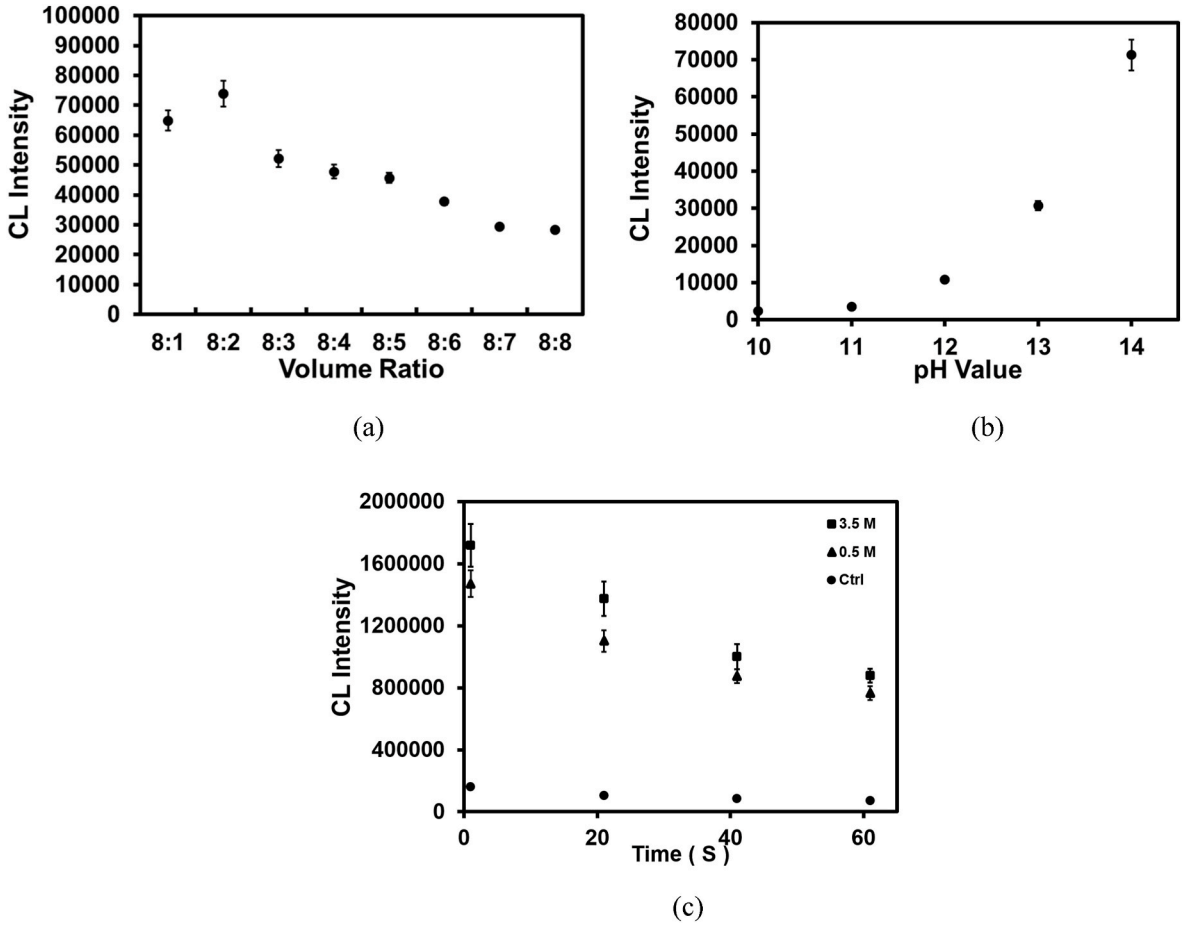

Fig. 5. Chemiluminescence intensity of the luminol-H_2O_2 reaction under various conditions. The chemiluminescence intensity of the luminol- H_2O_2 reaction with different (a) volume ratios of luminol- H_2O_2 ranging from 10 to 80 μL of H_2O_2 (50 mM) with a fixed volume of 80 μL of luminol (0.5 mM), (b) pH values of luminol (ranging from 10 to 14) with a fixed volume of 80 μL of luminol (0.5 mM) and 20 μL of H_2O_2 (50 mM), and (c) NaCl concentrations of AuNPs solution (0.5 and 3.5 M) with a fixed volume of 80 μL of luminol (0.5 mM, pH 14) and 20 μL of H_2O_2 (50 mM).

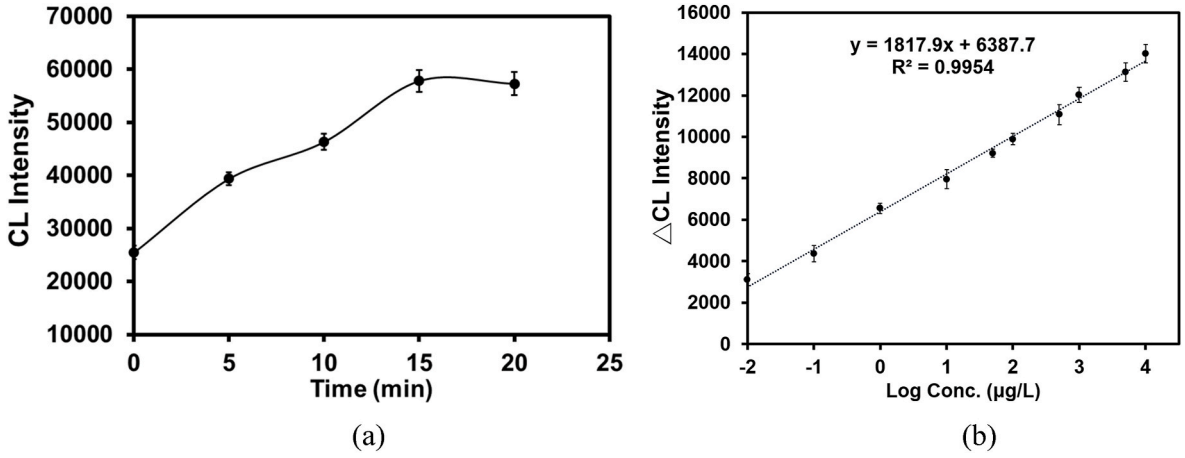

Fig. 6. Chemiluminescence signals of GLY detection using Apt-CL sensor. Chemiluminescence intensity of GLY detection using GBA aptamer at different (a) interaction time of 0, 5, 10,15, 20 and 25 min, and (b) concentrations (0.1–1.0 × 10^4 μg/L) of 15 min, under the optimal condition of AuNPs, GBA (0.1 μM), NaCl (3.5 M), H_2O_2 (50 mM), luminol (0.5 mM, pH 14) and luminol- H_2O_2 (v/v 4:1).

detect GLY in soil samples, which achieves sensitivity ranging from 0.08 to 1.9 μg/L, detecting levels as low as 0.05 μg/L, with a relative standard deviation (RSD) of 4.78–5.71% and a recovery ratio of 92.3–105.3% [28].

However, besides the use of AuNPs in this study, the synthesis of other fluorescent nanomaterials can be complicated and expensive. In contrast, the reaction between luminol and H_2O_2 requires no additional synthesis and is relatively inexpensive. In this study, the Apt-CL sensor displayed a strong linear correlation from 0.001 μg/L to 10 mg/L (LOD 0.0009 μg/L) in spiked soybean samples (Fig. 8). The aptamer-based

pesticide detection signal emitted a chemiluminescent response, enabling a significantly lower LOD and detection range for organophosphorus GLY compared to the aforementioned methods. The developed Apt-CL sensor can detect concentrations ranging from 0.001 μg/L to 10 mg/L with RSD between 1.44 and 2.58% and a recovery ratio of 79.6–81%. The Apt-CL sensor offered a broader measurement dynamic range and relatively stable deviation signals. Moreover, the reaction between luminol and H_2O_2 did not require extra synthesis and was relatively cost-effective.

Detecting GLY in soybeans presents challenges attributed to matrix content, such as fatty acids, proteins, and inorganic elements, contributing to decrease ionization, potential masking effects, and interference from the matrix [29]. Moreover, as glyphosate lacks a chromophore group, typical liquid chromatography detectors used for residue analysis must be employed, necessitating the initial derivatization of the analytes [30]. Although methods like LC-MS provide high accuracy, they entail intricate and time-consuming sample preparation procedures, including extraction, purification, derivatization, and concentration for both qualitative and quantitative testing, as well as instrument operation. Handling a large number of experimental samples may lead to elevated equipment costs, thereby impeding research efficiency.

Consequently, the Apt-CL sensor developed in this study offered a screening assay for detecting organophosphorus GLY with a lower LOD, and the linear range of detection concentration was also reduced by one order. The results of this study revealed that the chemiluminescent signal in this APT system originated from the luminol-H_2O_2 reaction. Both AuNPs and the aptamer itself lacked inherent chemiluminescence, ensuring no signal interference in the luminescent system. The Apt-CL sensor was successfully developed to capitalize on the specific binding capability of the aptamer to GLY, and the remaining aptamer molecules adsorbed onto the surface of AuNPs augmented the catalysis of the luminol-H_2O_2 chemiluminescent reaction through AuNPs aggregation. It indicated that Apt-CL sensor detected pesticide signals via chemiluminescent emission, ensuring high-sensitivity pesticide detection.

Even the gold standard analytical method for accurately detecting pesticide residues in food, was declared to use GC/LC-MS along with the QuEChERS extraction for matrix cleanup and pesticide extraction from crop matrix; however, it is both time and cost-consuming. Furthermore, GLY tends to be overlooked in routine screening bioassays for pesticides due to its AChE inhibition. The gold standard method does not include GLY among the 310 pesticides, primarily due to the initial derivatization required for GLY. This oversight makes it susceptible to being easily missed in confirmation detection. Except considering the influence of the crop matrix, we utilized the conventional GC/LC-MS method to detect GLY in water, aiming to compare the screening method with GLY detection in spiked agricultural products (Table S1). We observed that the screening method exhibited heightened detection sensitivity at lower concentrations. This was achieved by utilizing nanoparticle/aptamer capable of specific binding to GLY and amplifying the signal corresponding to the GLY concentration through fluorescence/chemiluminescence.

3.6. Specificity of GLY detection using Apt-CL sensor

In this study, the specificity of the Apt-CL sensor developed using the GBA molecular probe was investigated for the detection of 15 pesticides (1 mg/L) including GLY, chlorpyrifos, profenofos, cyhalothrin, cypermethrin, deltamethrin, lufenuron, tebufenozide, methomyl, chlorfenapyr, chlorantraniliprole, acetamiprid, imidacloprid, thiamethoxamand and dinotefuran. The chemiluminescence signals showed that GLY and profenofos can be clearly distinguished from the other 13 pesticides (Fig. 7). Interestingly, it was found that GBA can also bind to profenofos, which is also an organophosphorus pesticide [27]. A commonly used rapid screening assay for pesticides is the biochemical method that determines the inhibition of acetylcholinesterase (AChE) activity. However, GLY cannot inhibit the activity of AChE, making it difficult to detect using this method. Chlorpyrifos (64.6%) was most detected in the rapid biochemical screening method samples, followed by profenofos (22.4%) [31]. Therefore, the molecular probe aptamer GBA has the advantage of specific detection of GLY, which can effectively reduce the false positive cases in the biochemical method and improve the efficiency of chemical detection.

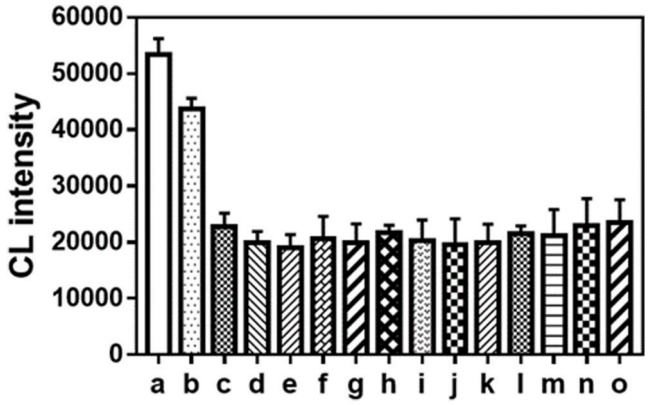

Fig. 7. Specificity detection of GBA aptamers. The luminescence signal generated by the luminol-H_2O_2 reaction was observed under the optimized experimental conditions at each pesticide concentration of 1 ppm. The pesticides are respectively as follows: a: GLY, b: profenofos, c: chlorpyrifos, d: ACP, e: imidamide, f: thiamethoxam, g: dinotefuran, h: cyhalothrin, i: cyhalothrin, j: deltamethrin, k: lufenuron, l: tebufenozide, m: methomyl, n: chlorfenapyr and o: chlorantraniliprole.

3.7. Determination of GLY in spiked soybean samples

This study aimed to evaluate the feasibility of using the Apt-CL sensor to determine GLY residues in soybean samples spiked with GLY. Soybean samples were immersed in GLY solutions with concentrations of 0, 1, 5, 20, 100, and 250 mg/L for 1 h. After extraction using the standard method for testing pesticide residues in food, the GLY concentration in the samples was determined by LC-MS/MS. The results showed that the residual GLY concentrations in the soybean samples were 0.19, 0.97, 3.88, 22.18, and 51.00 mg/L, respectively (Table 1). The results also indicated that the absorption ratio of GLY in soybeans was about 20%.

This study further detected GLY residues in GLY-spiked soybean samples using the Apt-CL sensor. Soybean samples were immersed in GLY solutions (0, 0.005, 0.01, 0.1, 1, 10, and 100 μg/L) and (1, 5, 10, 20, 50, 100, and 250 mg/L) for 1 h and extracted using the standard method of Test for Pesticide Residues in Foods. Based on the absorption ratio of 20%, the residual GLY concentrations were (0, 0.001, 0.002, 0.02, 0.2, 2, and 20 μg/L) and (0.2, 1, 2, 4, 10, 20, and 50 mg/L). The chemiluminescence intensity increased as the GLY residues increased, exhibiting a good linear relationship across the concentration range of 0.001 μg/L to 10 mg/L (Fig. 8). The detection range of the Apt-CL sensor covered the legal low standard specification for soybean, which is 10 mg/L or 20 mg/L.

As a systemic pesticide, GLY is more difficult to extract from crops compared to contact pesticides. Paraquat, another organophosphorus pesticide, is the second most commonly used herbicide after GLY worldwide [32], but unlike vegetables, the structure of the red bean seed coat lacks stomata and active transport mechanisms that can transport pesticides to the interior [31]. Systemic pesticide is easily absorbed by seed coat, and in most cases Paraquat would immediately attaches to the seed coat upon contact. According to the Standard Extraction Processes declared by the Taiwan Food and Drug Administration, this study prepared spiked soybean samples that were placed in GLY for 1 h before extraction. After extraction procedures, the results of LC-MS/MS detection (Table 1) showed that as the concentration of GLY was high,

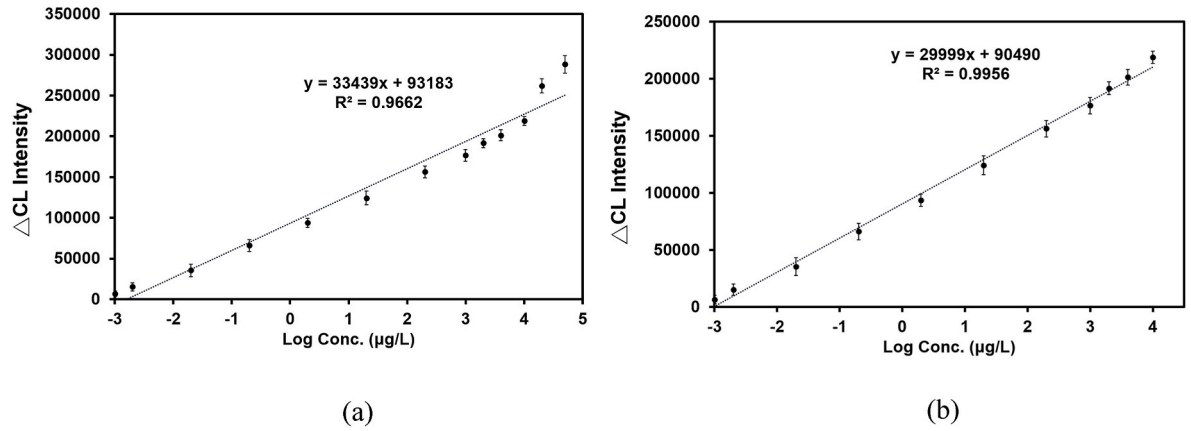

Fig. 8. Detection of GLY in spiked soybean samples. Chemiluminescence signals were detected from the spiked soybean samples soaked in GLY solutions (0, 0.005, 0.01, 0.1, 1, 10, and 100 μg/L) and (1, 5, 10, 20, 50, 100, and 250 mg/L) for 1 h after extraction. The standard curve was plotted using the chemiluminescence signals corresponding to absorption ratios of 20% for GLY concentrations of (a) 0, 0.001, 0.002, 0.02, 0.2, 2, and 20 μg/L and (b) 0.2, 1, 2, 4, 10, 20, and 50 mg/L.

Table 1
GLY residual concentration in GLY-spike soybean samples.

Concentration of GLY for soybean immersion (mg/L)	Residual concentration of GLY in soybeans[a] (mg/L)	Absorption	RSD[b]
0	ND	ND	ND
1	0.19	19.0%	1.86%
5	0.97	19.4%	2.60%
20	3.88	19.4%	1.44%
100	22.18	22.2%	1.56%
250	51.00	20.4%	2.12%

[a] LC-MS/MS.
[b] RSD: relative standard deviation.

the concentration of GLY in the matrix of processed soybeans increased accordingly with relative standard deviation ranging between 1.44% and 2.60%. Subsequently, the Apt-CL sensor developed in this study was used to test the extraction solution. The sensor had a high detected concentration range of 0.001 μg/L to 10 mg/L (Fig. 8b; R^2 0.9956, LOD 0.0009 μg/L. When the residual concentration exceeded 10 mg/L, the linear relationship between the luminescence intensity and the concentration was weak (Fig. 8a; R^2 0.9662), likely due to the excess accumulation of soybean matrix that affected the sensor signal. In contrast, when the detected concentration range was under the statutory specification of 10 mg/L, the linear relationship between the luminescence intensity and the concentration was strong (Fig. 8b).

In practice, routine screening bioassays for pesticides are frequently conducted in fruit and vegetable markets. If the residue exceeds the regulatory limit, subsequent gold standard testing is performed using the "Method of Test for Pesticide Residues in Foods – Multiresidue Analysis", which incorporated the QuEChERS extraction process coupled with GC-MS/MS or LC-MS/MS determination, enabling the simultaneous detection of 310 pesticide residues in agricultural products. However, GLY tends to be overlooked in routine screening bioassays for pesticides due to its weak AChE inhibition, and it is not included among the 310 pesticides covered by the standard method, primarily due to the initial derivatization required for GLY, making it susceptible to being easily missed in confirmation detection. Consequently, the "Method of Test for Pesticide Residues in Foods – Multiresidue Analysis of Polar Pesticides and their Metabolites" was developed to specifically address seven polar pesticides (GLY, glufosinate, 3-methylphosphinico propionic acid, N-Acetyl-glufosinate, ethephon, fosetyl-Al, and maleic hydrazide) found in grains and dry beans. Therefore, this study successfully achieved the goal of developing a screening method using the Apt-CL sensor for detecting GLY corresponding to concentrations in soybean samples ranging from 0.001 μg/L to 10 mg/L (LOD 0.0009 μg/L), which aligns with the regulatory values for GLY in various agricultural products (0.1–10 mg/L). The Apt-CL sensor is suggested for use as a sensitive screening method specifically for GLY, functioning as a primary screening tool with high specificity, simple operation procedures, short detection time, and low cost in application to rapid screening for crops sprayed with GLY. Upon obtaining a positive result in the screening method, further confirmation of pesticide residue is conducted using the standard method "Multiresidue Analysis of Polar Pesticides and their Metabolites". This study introduced the Apt-CL sensor as a feasible rapid screening method for quickly and accurately determining the presence of GLY in crops.

4. Conclusion

This study successfully developed an APT-CL sensor that utilized GBA aptamer as a molecular probe to specifically bind to GLY in soybeans through the luminol-H_2O_2 reaction catalyzed by AuNPs. The sensor has a detection limit of 0.01 μg/L and a linear range of 0.001 μg/L to 10 mg/L, enabling the detection of residual GLY in soybean samples. It meets the minimum requirement of 0.1 mg/L for GLY residue in agricultural crops according to Taiwan FDA regulations, as well as the EU and US EPA regulations for soybeans at 20 mg/L. The high specificity and user-friendly operation procedures make the APT-CL sensor as an ideal tool for farmers and regulatory agencies to quickly and accurately determine the presence of GLY in crops. Overall, the Apt-CL sensor is a valuable development to agricultural monitoring and management.

CRediT authorship contribution statement

Rui-Cian Weng: Writing – review & editing, Writing – original draft, Validation, Investigation, Data curation. **Min-Cheng Tsou:** Writing – original draft, Validation, Methodology, Investigation. **Jyun-Lin Lee:** Writing – review & editing, Investigation, Data curation. **Chao-Ming Tseng:** Methodology, Formal analysis. **Yu-Fen Huang:** Validation, Methodology, Formal analysis. **Yu-Lin Xiao:** Writing – review & editing, Validation. **Yen-Pei Lu:** Validation, Investigation. **Wei-Chun Chou:** Writing – review & editing. **Ruey-Feng Chang:** Writing – review & editing, Validation, Supervision. **Chun-Yu Chuang:** Writing – review & editing, Writing – original draft, Validation, Supervision, Data curation.

Declaration of competing interest

The authors declare that they have no known competing financial interests or personal relationships that could have appeared to influence the work reported in this paper.

Data availability

Data will be made available on request.

Acknowledgements

This study was funded by the National Science and Technology Council, Taiwan (grant No. NSTC 108-2622-E-007-013-CC2 110-2622-E-007-007). The authors thank the Instrumentation Center at National Tsing Hua University (NSTC 112-2740-M-007-001) for recording the TEM images.

Appendix A. Supplementary data

Supplementary data to this article can be found online at https://doi.org/10.1016/j.talanta.2024.125741.

References

[1] Food and Agriculture Organization of the united nations (Fao), Pesticides Use, 2020. https://www.fao.org/3/cc6958en/cc6958en.pdf.
[2] J.P. Myers, M.N. Antoniou, B. Blumberg, L. Carroll, T. Colborn, L.G. Everett, M. Hansen, P.J. Landrigan, B.P. Lanphear, R. Mesnage, L.N. Vandenberg, F.S. Vom Saal, W.V. Welshons, C.M. Benbrook, Concerns over use of glyphosate-based herbicides and risks associated with exposures: a consensus statement, Environ. Health 15 (2016) 19, https://doi.org/10.1186/s12940-016-0117-0.
[3] C.M. Benbrook, Trends in glyphosate herbicide use in the United States and globally, Environ. Sci. Eur. 28 (1) (2016) 3, https://doi.org/10.1186/s12302-016-0070-0.
[4] T. Bohn, M. Cuhra, T. Traavik, M. Sanden, J. Fagan, R. Primicerio, Compositional differences in soybeans on the market: glyphosate accumulates in roundup ready GM soybeans, Food Chem 153 (2014) 207–215, https://doi.org/10.1016/j.foodchem.2013.12.054.
[5] I. Heap, S.O. Duke, Overview of glyphosate-resistant weeds worldwide, Pest. Manag. Sci. 74 (5) (2018) 1040–1049, https://doi.org/10.1002/ps.4760.
[6] Markets, Markets, Biopesticides Market by Type, Source, Mode of Application, Formulation, Crop Application, and Region - Global Forecast to 2025, Biopesticides Market, 2020. https://www.marketsandmarkets.com/Market-Reports/biopesticides-267.html.
[7] G. Zhu, X. Chen, Aptamer-based targeted therapy, Adv. Drug Deliv. Rev. 134 (2018) 65–78, https://doi.org/10.1016/j.addr.2018.08.005.
[8] J. Fu, Y. Yao, X. An, G. Wang, Y. Guo, X. Sun, F. Li, Voltammetric determination of organophosphorus pesticides using a hairpin aptamer immobilized in a graphene oxide-chitosan composite, Mikrochim Acta 187 (1) (2019) 36, https://doi.org/10.1007/s00604-019-4022-4024.
[9] L. Wang, X. Liu, Q. Zhang, C. Zhang, Y. Liu, K. Tu, J. Tu, Selection of DNA aptamers that bind to four organophosphorus pesticides, Biotechnol. Lett. 34 (5) (2012) 869–874, https://doi.org/10.1007/s10529-012-0850-6.
[10] J. He, Y. Liu, M. Fan, X. Liu, Isolation and identification of the DNA aptamer target to acetamiprid, J. Agric. Food Chem. 59 (5) (2011) 1582–1586, https://doi.org/10.1021/jf104189g.
[11] F.X. Liu, X.W. Dou, Z.X. Yang, Q. Li, J.Y. Luo, Z.W. Fan, M.H. Yang, Advances on nanoparticles-tagged visual test strips for the rapid detection of pesticides, Zhongguo Zhong Yao Za Zhi 42 (16) (2017) 3056–3064, https://doi.org/10.19540/j.cnki.cjcmm.20170728.010.
[12] X. Li, R. Cheng, H. Shi, B. Tang, H. Xiao, G. Zhao, A simple highly sensitive and selective aptamer-based colorimetric sensor for environmental toxins microcystin-LR in water samples, J. Hazard. Mater. 304 (2016) 474–480, https://doi.org/10.1016/j.jhazmat.2015.11.016.
[13] H. Dong, C. Wang, Y. Xiong, H. Lu, H. Ju, X. Zhang, Highly sensitive and selective chemiluminescent imaging for DNA detection by ligation-mediated rolling circle amplified synthesis of DNAzyme, Biosens. Bioelectron. 41 (2013) 348–353, https://doi.org/10.1016/j.bios.2012.08.050.
[14] H. Hu, X. Liu, F. Jiang, X. Yao, X. Cui, A novel chemiluminescence assay of organophosphorous pesticide quinalphos residue in vegetable with luminol detection, Chem. Cent. J. 4 (2010) 13, https://doi.org/10.1186/1752-153X-4-13.
[15] Y. Gao, B. Li, Exonuclease III-assisted cascade signal amplification strategy for label-free and ultrasensitive chemiluminescence detection of DNA, Anal. Chem. 86 (17) (2014) 8881–8887, https://doi.org/10.1021/ac5024952.
[16] J.J. Storhoff, R. Elghanian, R.C. Mucic, C.A. Mirkin, R.L. Letsinger, One-pot colorimetric differentiation of polynucleotides with single base imperfections using gold nanoparticle probes, J. Am. Chem. Soc. 120 (9) (1998) 1959–1964, https://doi.org/10.1021/ja972332i.
[17] Y.F. Luo, L. He, S.S. Zhan, Y.G. Wu, L. Liu, W.T. Zhi, P. Zhou, Ultrasensitive resonance scattering (RS) spectral detection for trace tetracycline in milk using aptamer-coated nanogold (ACNG) as a catalyst, J. Agr. Food Chem. 62 (5) (2014) 1032–1037. https://pubs.acs.org/doi/10.1021/jf403566e.
[18] J.W. Liu, Adsorption of DNA onto gold nanoparticles and graphene oxide: surface science and applications, Phys. Chem. Chem. Phys. 14 (30) (2012) 10485–10496, https://doi.org/10.1039/C2CP41186E.
[19] L.H. Wang, X.F. Liu, X.F. Hu, S.P. Song, C.H. Fan, Unmodified gold nanoparticles as a colorimetric probe for potassium DNA aptamers, Chem. Commun. 36 (2006) 3780–3782, https://doi.org/10.1039/B607448K.
[20] X. Tao, F. He, X. Liu, F. Zhang, X. Wang, Y. Peng, J. Liu, Detection of chloramphenicol with an aptamer-based colorimetric assay: critical evaluation of specific and unspecific binding of analyte molecules, Mikrochim Acta 187 (12) (2020) 668, https://doi.org/10.1007/s00604-020-04644-6.
[21] K. Cho, Y. Lee, C.H. Lee, K. Lee, Y. Kim, H. Choi, P.D. Ryu, S.Y. Lee, S.W. Joo, Selective aggregation mechanism of unmodified gold nanoparticles in detection of single nucleotide polymorphism, J. Phys. Chem. C 112 (23) (2008) 8629–8633, https://doi.org/10.1021/jp801078m.
[22] Y.Y. Qi, F.R. Xiu, Sensitive and rapid chemiluminescence detection of propranolol based on effect of surface charge of gold nanoparticles, J. Lumin. 171 (2016) 238–245, https://doi.org/10.1016/j.jlumin.2015.11.013.
[23] Y.Y. Qi, F.R. Xiu, B.X. Li, One-step homogeneous non-stripping chemiluminescence metal immunoassay based on catalytic activity of gold nanoparticles, Anal. Biochem. 449 (2014) 1–8, https://doi.org/10.1016/j.ab.2013.12.007.
[24] Y.Y. Qi, F.R. Xiu, M.F. Zheng, B.X. Li, A simple and rapid chemiluminescence aptasensor for acetamiprid in contaminated samples: sensitivity, selectivity and mechanism, Biosens. Bioelectron. 83 (2016) 243–249, https://doi.org/10.1016/j.bios.2016.04.074.
[25] E.Y. Cheng, Y.B. Huang, M.Y. Chiang, Y.H. Hou, C.C. Nien, The study of pesticide residues control by the combination of AChE screening and chemical analysis: the Taipei model, J. Taiwan Agric. Res. 64 (1) (2015) 55–63, https://doi.org/10.6156/JTAR/2015.06401.06.
[26] P. Robouch, J. Stroka, J. Haedrich, A. Schaechtele, T. Wenzl, Guidance Document on the Estimation of LOD and LOQ for Measurements in the Field of Contaminants in Feed and Food, Publications Office of the European Union, 2016, https://doi.org/10.2787/8931.
[27] M. Jiang, C. Chen, J. He, H. Zhang, Z. Xu, Fluorescence assay for three organophosphorus pesticides in agricultural products based on magnetic-assisted fluorescence labeling aptamer probe, Food Chem 307 (2020) 125534, https://doi.org/10.1016/j.foodchem.2019.125534.
[28] Q.W. Liu, R. Zhang, B.G. Yu, A.H. Liang, Z.L. Jiang, A highly sensitive gold nanosol SERS aptamer assay for glyphosate with a new COF nanocatalytic reaction of glycol-au(III), Sens. Actuators B Chem. 344 (2021) 130288, https://doi.org/10.1016/j.snb.2021.130288.
[29] B. Gilbert-Lopez, J.F. Garcia-Reyes, A. Molina-Diaz, Sample treatment and determination of pesticide residues in fatty vegetable matrices: a review, Talanta 79 (2) (2009) 109–128, https://doi.org/10.1016/j.talanta.2009.04.022.
[30] N. Chamkasem, T. Harmon, Direct determination of glyphosate, glufosinate, and AMPA in soybean and corn by liquid chromatography/tandem mass spectrometry, Anal. Bioanaly. Chem. 408 (18) (2016) 4995–5004, https://doi.org/10.1007/s00216-016-9597-6.
[31] F. Chen, Y. Ye, B. Jin, B. Yi, Q. Wei, L. Liao, Homicidal paraquat poisoning, J. Forensic. Sci. 64 (3) (2019) 941–945, https://doi.org/10.1111/1556-4029.13945.
[32] C.M. Tsen, C.W. Yu, W.C. Chuang, M.J. Chen, S.K. Lin, T.H. Shyu, Y.H. Wang, C. C. Li, W.C. Chao, C.Y. Chuang, A simple approach for the ultrasensitive detection of paraquat residue in adzuki beans by surface-enhanced Raman scattering, Analyst 144 (2) (2019) 426–438, https://doi.org/10.1039/c8an01845f.